

Spin density wave and superconductivity in the bilayer t - J model of $\text{La}_3\text{Ni}_2\text{O}_7$ under renormalized mean-field theory

Yang Tian¹ and Yan Chen^{1,2,*}

¹*Department of Physics and State Key Laboratory of Surface Physics, Fudan University, Shanghai 200433, China*

²*Shanghai Branch, Hefei National Laboratory, Shanghai 201315, China*

(Dated: December 24, 2024)

Motivated by the recently discovered bilayer nickelate superconductor, the pressurized $\text{La}_3\text{Ni}_2\text{O}_7$, we present a renormalized mean-field theory of a bilayer single-band t - J model, highlighting the interplay between magnetism and superconductivity. We analyze the pairing symmetry and magnetic properties of the system, predicting two distinct states in which magnetism and superconductivity coexist. As hole doping increases, the magnetic order is rapidly suppressed. The inter-layer hopping t_\perp and coupling J_\perp promote a transition from intra-layer d -wave pairing to s -wave pairing, which is accompanied by a shift from antiferromagnetic (AFM) order to a double spin stripe configuration. The latter has been extensively observed in ambient and high-pressure experiments. Our study offers theoretical insights into the coexistence of spin density waves and superconductivity.

I. INTRODUCTION

The discovery of unconventional superconductivity in the Ruddlesden-Popper (RP) series of nickel-based oxides, denoted as $R_{n+1}\text{Ni}_n\text{O}_{3n+1}$ where R represents a rare earth element and N indicates the number of consecutive layers, has attracted significant attention. Superconductivity has been observed at approximately 80 K in $\text{La}_3\text{Ni}_2\text{O}_7$ [1–4] and around 30 K in $\text{La}_4\text{Ni}_3\text{O}_{10}$ [5–9] under high pressure. However, the mechanisms underlying superconductivity in these materials remain a subject of ongoing investigations. Additionally, the $\text{La}_3\text{Ni}_2\text{O}_7$ may exhibit a more complex ordered phase because of the alternating hole distribution between Ni^{2+} and Ni^{3+} , which may lead to a charge density wave (CDW) and spin density wave (SDW).

Due to their similarities with cuprates, the interplay between superconductivity and magnetism is a crucial issue in the study of unconventional superconductors, particularly nickelates. Recent experiments provide a density-wave-like transition in $\text{La}_3\text{Ni}_2\text{O}_{7-\delta}$ at ambient pressure[4, 10–18]. The density wave is highly suppressed with increasing pressure, suggesting a competition with superconductivity. The resonant inelastic X-ray scattering (RIXS)[10], nuclear magnetic resonance (NMR)[11, 12], resonant soft X-ray scattering (RSXS)[13] and μsR [14, 15] measurements suggest a SDW transition around $T_{SDW} \approx 150\text{K}$, with a vector of $(0.5\pi, 0.5\pi)$. The magnetic ordering temperature increases by the pressure and approaches 155K at 2.31GPa[15]. The ultrafast optical pump-probe spectroscopy measurements provide a density-wave-like order at high pressure[18]. They proposed that the SDW observed at ambient pressure is gradually suppressed up to 13.3 GPa and completely vanishes around 26 GPa. Besides that, a distinct density-wave-like order emerges at

pressures exceeding 29.4 GPa, with a transition temperature of approximately 135 K, likely associated with the predicted CDW order.

There are many theoretical works for the bilayer nickelate $\text{La}_3\text{Ni}_2\text{O}_7$ [7, 19–41]. Most researchers believe that superconductivity primarily arises from the two e_g orbitals ($d_{x^2-y^2}$ and $d_{3z^2-r^2}$). The $d_{x^2-y^2}$ orbital is nearly quarter-filled, while the $d_{3z^2-r^2}$ orbital is close to half-filled. The $d_{3z^2-r^2}$ orbitals are strongly coupled via inter-layer superexchange interactions mediated by the O - $2p_z$ orbital. Furthermore, these two $3d$ orbitals interact through onsite Hund’s coupling, which transfers the strong inter-layer antiferromagnetic (AFM) coupling from the $d_{3z^2-r^2}$ orbital to the $d_{x^2-y^2}$ orbital[30, 37, 42]. Based on these facts, various multi-band and single-band models have been developed, predicting s_\pm -wave and d -wave pairing states. Apart from superconductivity, experimental investigations of density waves have revealed various spin- and charge-ordered states, which is also confirmed by several theoretical studies [41, 43–48]. Some investigations argue that these states compete with superconductivity, suggesting that magnetic fluctuations could provide essential understanding for the pairing mechanisms behind high-temperature superconductivity in nickelates.

The linear spin density wave theory of a Heisenberg model with the third-nearest-neighbor AFM exchange coupling suggests several magnetic structures[10, 11], where the effective inter-layer magnetic superexchange interaction is more substantial than the intra-layer magnetic interactions. The most likely spin configuration among the various magnetic structures, named the “double spin stripe,” is characterized by the ferromagnetic alignment of Ni atom spins in the x - y direction and the alternating antiferromagnetic alignment in the x - y direction. This stripe phase has been corroborated by other explorations employing various methods[13, 46, 47]. Furthermore, certain studies assert the existence of spin stripes in the absence of significant charge disproportionation[13]. However, this stripe phase was

* yanchen99@fudan.edu.cn

identified in the normal state of $\text{La}_3\text{Ni}_2\text{O}_7$, and the interplay between the SDW and superconductivity remains unexplored.

We investigate a bilayer single-band t - J model for $\text{La}_3\text{Ni}_2\text{O}_7$ using renormalization mean-field theory (RMFT) to identify potential density wave orders and superconductivity. In the mean-field framework, we introduce four variational order parameters: the hole density δ_{li} , the local spin moment representing antiferromagnetic correlations, the pair field $\Delta_{ij\sigma}$ indicating local electron pairing, and the bond order corresponding to the kinetic hopping term, where i denotes a site position and $\langle ij \rangle$ represents the nearest-neighbor bond. An iterative method is employed to solve the mean-field Hamiltonian H_{MF} for all parameters, requiring potentially over 1000 iterations. Convergence is achieved for each order parameter when its value changes by less than 10^{-3} between successive iterations. All calculations are performed on an 8×8 square lattice, with specific patterns of δ_{li} used as initial values to obtain various charge orders. In contrast, bond orders are assumed to be uniform initially. At low doping, we identify a double spin stripe state characterized by the wave vector $Q = (\pi/2, \pi/2)$ and demonstrate that the inter-layer pairing of $d_{x^2-y^2}$ orbitals predominates and coexists with the SDW. Furthermore, the intra-layer pairing competes with the inter-layer pairing, which increases inter-layer superexchange magnetic coupling.

II. MODEL HAMILTONIAN AND METHODS

We start from the single-band t - J model on a bilayer square lattice of the Ni-O plane, given by $H = H_{\parallel} + H_{\perp}$:

$$\begin{aligned} H_{\parallel} &= -t \sum_{\langle ij \rangle, l, \sigma} (c_{li\sigma}^{\dagger} c_{lj\sigma} + h.c.) + J_1 \sum_{\langle ij \rangle, l} \mathbf{S}_{li} \cdot \mathbf{S}_{lj} \\ &\quad + J_2 \sum_{\langle\langle ij \rangle\rangle, l} \mathbf{S}_{li} \cdot \mathbf{S}_{lj} \\ H_{\perp} &= -t_{\perp} \sum_{i, \sigma} (c_{1i\sigma}^{\dagger} c_{2i\sigma} + h.c.) + J_{\perp} \sum_i \mathbf{S}_{1i} \cdot \mathbf{S}_{2i}, \end{aligned} \quad (1)$$

where $l = 1, 2$ labels the top and bottom layers, and $c_{li\sigma}^{\dagger}$ creates an electron at site i with spin σ on layer l . $S_{li} = \frac{1}{2} \sum_{\alpha\beta} c_{li\alpha}^{\dagger} \sigma_{\alpha\beta} c_{li\beta}$ is the spin operator. t and t_{\perp} is the hopping amplitude of intra-layer and inter-layer nearest-neighbor electrons, respectively. The nearest-neighbor hopping t is set to be the energy unit. The three magnetic exchange couplings J_1 , J_2 and J_{\perp} respectively represent the nearest-neighbor of intra-layer exchange interaction, third nearest-neighbor of the intra-layer exchange interaction, and nearest-neighbor of inter-layer exchange interaction.

The strong coupling constraint of no double occupancy is hard to study analytically. Zhang *et al* introduced Gutzwiller renormalization factors to treat the constraint approximately[49]. Later, the antiferromagnetic (AFM)

order case was considered by Himeda and Ogata[50]. The resulting renormalized Hamiltonian is

$$\begin{aligned} H &= H'_{\parallel} + H'_{\perp} \\ H'_{\parallel} &= -t \sum_{\langle ij \rangle, l, \sigma} g_{lij\sigma}^t (c_{li\sigma}^{\dagger} c_{lj\sigma} + h.c.) \\ &\quad + J_1 \sum_{\langle ij \rangle, l} (g_{lij}^{s,z} \mathbf{S}_{li}^z \mathbf{S}_{lj}^z + g_{lij}^{s,xy} (\frac{\mathbf{S}_{li}^+ \mathbf{S}_{lj}^- + \mathbf{S}_{li}^- \mathbf{S}_{lj}^+}{2})) \\ &\quad + J_2 \sum_{\langle\langle ij \rangle\rangle, l} (g_{lij}^{s,z} \mathbf{S}_{li}^z \mathbf{S}_{lj}^z + g_{lij}^{s,xy} (\frac{\mathbf{S}_{li}^+ \mathbf{S}_{lj}^- + \mathbf{S}_{li}^- \mathbf{S}_{lj}^+}{2})) \\ H'_{\perp} &= -t_{\perp} \sum_{i, \sigma} g_{ii\sigma\perp}^t (c_{1i\sigma}^{\dagger} c_{2i\sigma} + h.c.) \\ &\quad + J_{\perp} \sum_i (g_{ii\perp}^{s,z} \mathbf{S}_{1i}^z \mathbf{S}_{2i}^z + g_{ii\perp}^{s,xy} (\frac{\mathbf{S}_{1i}^+ \mathbf{S}_{2i}^- + \mathbf{S}_{1i}^- \mathbf{S}_{2i}^+}{2})) \end{aligned} \quad (2)$$

The renormalization factors g^t and g^s used to evaluate a projected mean field wave function depend on local values of the magnetic and pairing order parameters, and the local mean field parameters are defined as:

$$\begin{aligned} m_{li}^{\nu} &= \langle \Psi_0 | S_{li}^z | \Psi_0 \rangle \\ \Delta_{lij\sigma}^{\nu} &= \sigma \langle \Psi_0 | c_{li\sigma} c_{lj\sigma} | \Psi_0 \rangle \\ \chi_{lij\sigma}^{\nu} &= \langle \Psi_0 | c_{li\sigma}^{\dagger} c_{lj\sigma} | \Psi_0 \rangle \\ \delta_{li} &= 1 - \langle \Psi_0 | n_{li} | \Psi_0 \rangle \end{aligned} \quad (3)$$

where $\langle \Psi_0 |$ is the unprojected wave function. The superscript ν denotes that these quantities are unprojected and different from the real physical quantities. δ_{li} , $\Delta_{lij\sigma}^{\nu}$ and $\chi_{lij\sigma}^{\nu}$ are hole density, pairing amplitude on layer l , and hopping amplitude, respectively. The original form of the Gutzwiller factors introduced by Himeda and Ogata are complicated[50]. We use the simpler form as follows:

$$\begin{aligned} g_{lij\sigma}^t &= g_{li\sigma}^t g_{lj\sigma}^t \\ g_{li\sigma}^t &= \sqrt{\frac{2\delta_{li}(1-\delta_{li})}{1-\delta_{li}^2+4(m_{li}^{\nu})^2}} \frac{1+\delta_{li}+\sigma 2m_{li}^{\nu}}{1+\delta_{li}-\sigma 2m_{li}^{\nu}} \\ g_{lij}^{s,xy} &= g_{li}^{s,xy} g_{lj}^{s,xy} \\ g_{li}^{s,xy} &= \frac{2\delta_{li}(1-\delta_{li})}{1-\delta_{li}^2+4(m_{li}^{\nu})^2} \\ g_{lij}^{s,z} &= g_{lij}^{s,xy} \frac{2((\bar{\Delta}_{lij}^{\nu})^2 + (\bar{\chi}_{lij}^{\nu})^2) - 4m_{li}^{\nu} m_{lj}^{\nu} X_{ij}^2}{2((\bar{\Delta}_{lij}^{\nu})^2 + (\bar{\chi}_{lij}^{\nu})^2) - 4m_{li}^{\nu} m_{lj}^{\nu}} \\ X_{ij} &= 1 + \frac{12(1-\delta_{li})(1-\delta_{lj})((\bar{\Delta}_{lij}^{\nu})^2 + (\bar{\chi}_{lij}^{\nu})^2)}{\sqrt{(1-\delta_{li}^2+4(m_{li}^{\nu})^2)(1-\delta_{lj}^2+4(m_{lj}^{\nu})^2)}} \end{aligned} \quad (4)$$

where $\bar{\Delta}_{lij}^{\nu} = \sum_{l\sigma} \frac{\Delta_{lij\sigma}^{\nu}}{2}$ and $\bar{\chi}_{lij}^{\nu} = \sum_{l\sigma} \frac{\chi_{lij\sigma}^{\nu}}{2}$. The Gutzwiller factors and mean field parameters can give the ground state energy of renormalized Hamiltonian,

$$\begin{aligned}
E &= \langle \Psi_0 | H' | \Psi_0 \rangle \\
&= -t \sum_{\langle ij \rangle, \sigma}^{l=1,2} g_{lij\sigma}^t (\chi_{lij\sigma}^\nu + h.c.) - J_1 \sum_{\langle ij \rangle, \sigma}^{l=1,2} \left(\left(\frac{g_{lij}^{s,z}}{4} + \frac{g_{lij}^{s,xy}}{2} \frac{\Delta_{lij\bar{\sigma}}^{\nu*}}{\Delta_{lij\sigma}^{\nu*}} \right) \Delta_{lij\sigma}^{\nu*} \Delta_{lij\sigma}^\nu + \left(\frac{g_{lij}^{s,z}}{4} + \frac{g_{lij}^{s,xy}}{2} \frac{\chi_{lij\bar{\sigma}}^{\nu*}}{\chi_{lij\sigma}^{\nu*}} \right) \chi_{lij\sigma}^{\nu*} \chi_{lij\sigma}^\nu \right) + J_1 \sum_{\langle ij \rangle}^{l=1,2} g_{lij}^{s,z} m_{li}^\nu m_{lj}^\nu \\
&\quad - J_2 \sum_{\langle\langle ij \rangle\rangle, \sigma}^{l=1,2} \left(\left(\frac{g_{lij}^{s,z}}{4} + \frac{g_{lij}^{s,xy}}{2} \frac{\Delta_{lij\bar{\sigma}}^{\nu*}}{\Delta_{lij\sigma}^{\nu*}} \right) \Delta_{lij\sigma}^{\nu*} \Delta_{lij\sigma}^\nu + \left(\frac{g_{lij}^{s,z}}{4} + \frac{g_{lij}^{s,xy}}{2} \frac{\chi_{lij\bar{\sigma}}^{\nu*}}{\chi_{lij\sigma}^{\nu*}} \right) \chi_{lij\sigma}^{\nu*} \chi_{lij\sigma}^\nu \right) + J_2 \sum_{\langle\langle ij \rangle\rangle}^{l=1,2} g_{lij}^{s,z} m_{li}^\nu m_{lj}^\nu \\
&\quad - t_\perp \sum_{i,\sigma} g_{ii\sigma\perp}^t (\chi_{i\sigma\perp}^\nu + h.c.) - J_\perp \sum_{i,\sigma} \left(\left(\frac{g_{ii\perp}^{s,z}}{4} + \frac{g_{ii\perp}^{s,xy}}{2} \frac{\Delta_{i\sigma\perp}^{\nu*}}{\Delta_{i\sigma}^{\nu*}} \right) \Delta_{i\sigma\perp}^{\nu*} \Delta_{i\sigma\perp}^\nu + \left(\frac{g_{ii\perp}^{s,z}}{4} + \frac{g_{ii\perp}^{s,xy}}{2} \frac{\chi_{i\sigma\perp}^{\nu*}}{\chi_{i\sigma}^{\nu*}} \right) \chi_{i\sigma\perp}^{\nu*} \chi_{i\sigma\perp}^\nu \right) + J_\perp \sum_i g_{ii\perp}^{s,z} m_{1i}^\nu m_{2i}^\nu
\end{aligned} \tag{5}$$

Then we need to minimize the energy with two constraints: $\sum_i n_i = Ne$ and $\langle \Psi_0 | \Psi_0 \rangle = 1$. We use the Lagrangian multiplier procedure to obtain the target function:

$$\begin{aligned}
W &= \langle \Psi_0 | H' | \Psi_0 \rangle - \lambda (\langle \Psi_0 | \Psi_0 \rangle - 1) \\
&\quad - \mu \left(\sum_i n_i - Ne \right)
\end{aligned} \tag{6}$$

The mean field Hamiltonian is given by $H_{MF} | \Psi_0 \rangle = \lambda | \Psi_0 \rangle$ and becomes

$$\begin{aligned}
H_{MF} &= \sum_{ij,l,\sigma} \frac{\partial W}{\partial \chi_{lij\sigma}^\nu} c_{li\sigma}^\dagger c_{lj\sigma} + h.c. \\
&\quad + \sum_{ij,l,\sigma} \frac{\partial W}{\partial \Delta_{lij\sigma}^\nu} \sigma c_{li\sigma} c_{lj\sigma} + h.c. + \sum_{l,i,\sigma} \frac{\partial W}{\partial n_{li\sigma}} n_{li\sigma}
\end{aligned} \tag{7}$$

The coefficients above are given as

$$\begin{aligned}
\frac{\partial W}{\partial \chi_{lij\sigma}^\nu} &= -J_p \left(\frac{g_{lij}^{s,z}}{4} + \frac{g_{lij}^{s,xy}}{2} \frac{\chi_{lij\bar{\sigma}}^{\nu*}}{\chi_{lij\sigma}^{\nu*}} \right) \chi_{lij\sigma}^{\nu*} - t g_{lij\sigma}^t \\
&\quad + \frac{\partial W}{\partial g_{lij}^{s,z}} \frac{\partial g_{lij}^{s,z}}{\partial \chi_{lij\sigma}^\nu} \\
\frac{\partial W}{\partial \Delta_{lij\sigma}^\nu} &= -J_p \left(\frac{g_{lij}^{s,z}}{4} + \frac{g_{lij}^{s,xy}}{2} \frac{\Delta_{lij\bar{\sigma}}^{\nu*}}{\Delta_{lij\sigma}^{\nu*}} \right) \Delta_{lij\sigma}^{\nu*} + \frac{\partial W}{\partial g_{lij}^{s,z}} \frac{\partial g_{lij}^{s,z}}{\partial \Delta_{lij\sigma}^\nu} \\
\frac{\partial W}{\partial n_{i\sigma}} &= -\mu - \frac{1}{2} \sigma \sum_j g_{lij}^{s,z} J_p m_{lj}^\nu - \sum_j \frac{\partial W}{\partial g_{lij}^{s,xy}} \frac{\partial g_{lij}^{s,xy}}{\partial n_{i\sigma}} \\
&\quad - \sum_j \frac{\partial W}{\partial g_{lij}^{s,z}} \frac{\partial g_{lij}^{s,z}}{\partial n_{i\sigma}} - \sum_{j\sigma'} \frac{\partial W}{\partial g_{lij\sigma'}^t} \frac{\partial g_{lij\sigma'}^t}{\partial n_{i\sigma}}
\end{aligned} \tag{8}$$

where J_p represents all the magnetic coupling from Eq.(1). This mean-field Hamiltonian H_{MF} can be solved self-consistently; the eigenvalues and eigenvectors can determine the final mean-field parameters defined in Eq.(3). After the self-consistency is achieved, we calculate the or-

der parameters:

$$\begin{aligned}
\Delta_{\parallel,i} &= \sum_\sigma (g_{li,\sigma}^t g_{li+x,\bar{\sigma}}^t \Delta_{li,i+x,\sigma}^\nu + g_{li,\sigma}^t g_{li-x,\bar{\sigma}}^t \Delta_{li,i+x,\sigma}^\nu \\
&\quad + g_{li,\sigma}^t g_{li+y,\bar{\sigma}}^t \Delta_{li,i+y,\sigma}^\nu + g_{li,\sigma}^t g_{li-y,\bar{\sigma}}^t \Delta_{li,i-y,\sigma}^\nu) / 8, \\
\Delta_{\perp,i} &= \sum_\sigma g_{li,\sigma}^t g_{li+z,\bar{\sigma}}^t \Delta_{li,i+z,\sigma}^\nu, \\
m_{li} &= (\sqrt{g_{li,i+x}^{s,z}} + \sqrt{g_{li,i-x}^{s,z}} + \sqrt{g_{li,i+y}^{s,z}} + \sqrt{g_{li,i-y}^{s,z}} \\
&\quad + \sqrt{g_{li,i+2x}^{s,z}} + \sqrt{g_{li,i-2x}^{s,z}} + \sqrt{g_{li,i+2y}^{s,z}} + \sqrt{g_{li,i-2y}^{s,z}} \\
&\quad + \sqrt{g_{li,i+z}^{s,z}}) m_{li}^\nu / 9,
\end{aligned} \tag{9}$$

III. NUMERICAL RESULTS

We adopt typical values of $t = 1, J_1 = 0.3, J_2 = 0.2$, and focusing on the influence of inter-layer hopping t_\perp and J_\perp . The size of the system is 8×8 . Then we employ an iterative method to achieve a self-consistent solution for Eq.(7), continuing the process until the mean field parameters Eq.(3) difference between two successive iterations is less than 10^{-3} . To obtain all possible various magnetic orders, we input specific patterns of δ_{li}, m_{li}^ν and $\Delta_{lij\sigma}^\nu$ as initial values except the bond orders $\chi_{lij\sigma}^\nu$ which are always initially assumed to be uniform. We obtain only uniform pairing order parameters, such as the intra-layer d -wave superconducting and coexistent anti-ferromagnetic states. The absolute values of the upper and lower order parameters are equivalent, allowing us to omit the layer label l . Besides, the coexistence of intra-layer s -wave superconducting state and double spin stripe survive at large inter-layer hopping and coupling.

Thus, we can define superconducting order parameters and magnetic order parameters as follows:

$$\begin{aligned}
\Delta_{\parallel} &= \Delta_{\parallel,i} = \Delta_{\parallel}^s + i \Delta_{\parallel}^d, \\
\Delta_{\perp} &= \Delta_{\perp,i}, \\
m_{AF} &= \frac{1}{\sqrt{N}} \sum_k m_i e^{-i\pi R_{ix,iy}}, \\
m_{DS} &= \frac{1}{\sqrt{N}} \sum_k m_i e^{-i\frac{\pi}{2} R_{ix,iy}},
\end{aligned} \tag{10}$$

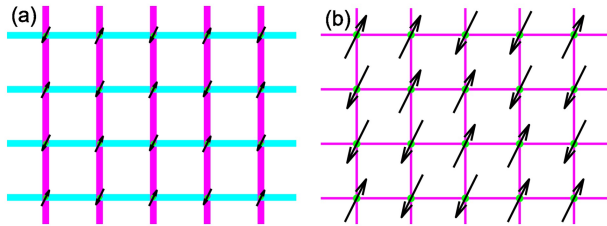


FIG. 1. Schematic illustration of modulations for stripe like patterns. (a) d -wave pairing and AFM with doping $\delta = 0.1$ (b) s -wave and double spin stripe with doping $\delta = 0.15$, respectively. The size of the green circle represents the hole density. The bond width around each site represents the amplitude of the superconducting order parameter, and the sign is positive (negative) for blue (red). The size of the black arrows represents the spin moment.

A. Magnetism and superconductivity coexistence states

In addition to the antiferromagnetism (AFM), we obtain double spin tripe with a period of four lattice spaces ($4a_0$), which consists of an up/up/down/down pattern of diagonal stripes. Both of them can coexist with superconductivity. Fig.1 shows a schematic illustration of the pair field, charge density, and spin moment for the two magnetism and superconductivity coexistence states with a hole concentration of Fig.1(a) and 0.15 Fig.1(b). The magnitude of the pair field is proportional to the width of the bond; blue (red) denotes a positive (negative) value. The size of the arrow is proportional to the spin moment, and the size of the circle represents the hole density. Both charge and pairing are uniform. The antiferromagnetic (AFM) coexists with intra-layer d -wave pairing, and the double spin stripe coexists with s -wave pairing.

It is known that the coexistence of uniform d -wave pairing superconductivity and AFM is stable in the t - J model. The third nearest neighbor coupling $J_2 > 0$ competes with J_1 , leading to a double spin stripe state and breaking AFM simultaneously. The stripe is also inseparable from the bilayer structure, so it coexists with s -wave pairing and inter-layer pairing. Those two pairings also compete with d -wave pairing.

B. Doping effect

Superconducting pairing and magnetic as a function of hole doping level with different t_\perp and J_\perp are displayed in Fig.2. At $t_\perp = 0, J_\perp = 0$, there is only intra-layer d -wave pairing Δ_\parallel^d because each layer is an individual t - J model, see in Fig.2(a). Due to the existence of J_2 , there is a tiny double spin stripe order, and the amplitude of this stripe is less than 10^{-5} . Compared to the AFM

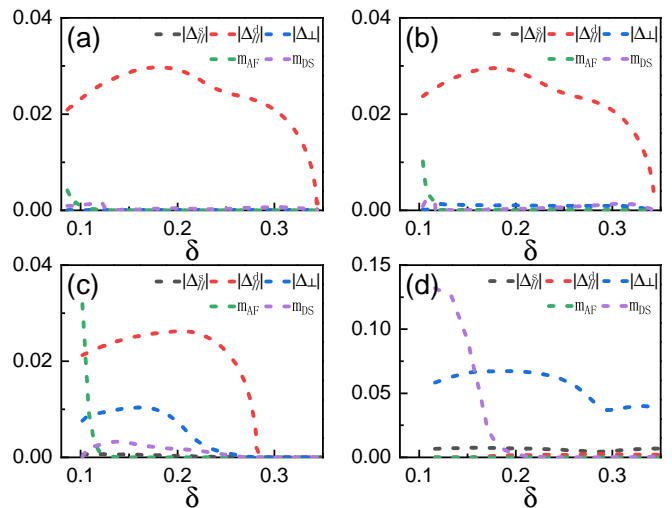


FIG. 2. Superconducting pairing and magnetic order parameter as a function of hole doping δ for (a) $t_\perp = 0, J_\perp = 0$ (b) $t_\perp = 0, J_\perp = 0.3$ (c) $t_\perp = 0.5, J_\perp = 0.3$ (d) $t_\perp = 0.5, J_\perp = 0.5$. The intra-layer s -wave pairing exists only in nonzero t_\perp and J_\perp . The double spin stripe mainly coexists with the inter-layer pairing.

order found in the t - J model with only nearest neighbor magnetic interaction, m_{AF} is much smaller. Still, the superconducting order parameter is more significant and exists in a broader range of δ . This may be understood as the consequence of the nonzero value of J_2 in the present case, which competes with J_1 , leading to a smaller AFM order.

The order parameters as a function of δ at $J_\perp = 0.3$ are depicted in Fig.2(b). In this case, two layers are antiferromagnetically coupled by J_\perp . The intra-layer d -wave pairing Δ_\parallel^d is almost unchanged from that in Fig. 2(a), and the inter-layer pairing Δ_\perp arises and stays around 10^{-3} . The AFM order at low doping increases due to the contribution of the last term in Eq.(5). The double spin stripe order is around 10^{-4} , so we approximate that it does not coexist with the d -wave pairing.

In Fig.2(c), we display the order parameters as a function of δ at $t_\perp = 0.5, J_\perp = 0.3$. At finite doping, the intra-layer s -wave pairing Δ_\parallel^s appears, leading to an in-plane $s+id$ -wave pairing with an inter-layer pairing which is also reported by Wu *et al* [37]. The intra-layer d -wave pairing Δ_\parallel^d is suppressed but still the dominant pairing. The inter-layer pairing Δ_\perp increases to around 0.01 with t_\perp is up to 0.5. This may explain the observed superconductivity in $\text{La}_3\text{Ni}_2\text{O}_7$ under pressure. At low doping, the ground state has AFM order. As δ increases, the magnetism becomes a double spin stripe, and AFM vanishes. It is interesting to note that the intra-layer s -wave pairing Δ_\parallel^s survives only with nonzero values of t_\perp and J_\perp , and Δ_\parallel^s has opposite signs with inter-layer pairing Δ_\perp . These may be explained by the fact that Δ_\parallel^s comes from the inter-layer pairing, which also can be interpreted by

Eq.(21).

We plot the the order parameters for $t_{\perp} = 0.5, J_{\perp} = 0.5$ in Fig.2(d). The intra-layer d -wave pairing Δ_{\parallel}^d is further suppressed at a larger J_{\perp} , the inter-layer pairing Δ_{\perp} becomes the dominant pairing at the same time. Δ_{\parallel}^s increases as well, confirming the previous explanation. The inter-layer pairing Δ_{\perp} changes nonmonotonically concerning different doping levels, similar to doped two-leg spin-1/2 and spin-1 ladder[50]. This may be the feature of bilayer or two-leg system[51, 52]. As we can see, the double spin stripe increases rapidly, and AFM is completely suppressed. This gives rise to a coexistence state of intra-layer s -wave pairing Δ_{\parallel}^s , inter-layer pairing Δ_{\perp} and double spin stripe.

C. Analysis of pairing symmetry

To give a further analysis of the problem, we switch to k space to obtain some relations between the mean fields. The mean-field Hamiltonian Eq.(7) can be written in momentum space as

$$H_k = \sum_{k,\sigma} \epsilon_k c_{k,\sigma}^{\dagger} c_{k,\sigma}^{\dagger} + \sum_k \tilde{\Delta}_k c_{k\uparrow}^{\dagger} c_{-k\downarrow}^{\dagger} + h.c. \quad (11)$$

where

$$\begin{aligned} \epsilon_{k_1} = & -2g_t t (\cos k_x + \cos k_y) - g_t t_{\perp} \cos k_z \\ & - \frac{3}{4} g_s J_1 (2\chi_x \cos k_x + 2\chi_y \cos k_y) \\ & - \frac{3}{4} g_s J_2 (2\chi'_x \cos 2k_x + 2\chi'_y \cos 2k_y) \\ & - \frac{3}{4} g_s J_{\perp} \chi_z \cos k_z \end{aligned} \quad (12)$$

$$\begin{aligned} \tilde{\Delta}_{k_1} = & -\frac{3}{4} g_s J_1 (2\Delta_x \cos k_x + 2\chi_y \cos k_y) \\ & - \frac{3}{4} g_s J_2 (2\Delta'_x \cos 2k_x + 2\Delta'_y \cos 2k_y) \\ & - \frac{3}{4} g_s J_{\perp} \Delta_z \cos k_z \end{aligned} \quad (13)$$

$$\epsilon_k = 2\epsilon_{k_1}, \quad \tilde{\Delta}_k = 2\tilde{\Delta}_{k_1} \quad (14)$$

ϵ_{k_1} and $\tilde{\Delta}_{k_1}$ is the corresponding energy of layer 1. The mean fields of layer 2 are the same as those of layer 1. Within the range of values in this article, J_2 does not affect the pairing symmetry, see in Fig.3, and neither does magnetism. Thus we can set $J_2 = 0, J_{\perp} = J_1$ to analyze the pairing symmetry. We consider the half-filled case with $g_t = 0$. The total energy of the system is

$$E = -\frac{3}{4} g_s J_1 \sum_k E_k \quad (15)$$

where

$$E_k = \sqrt{\chi_k^2 + \Delta_k^2} \quad (16)$$

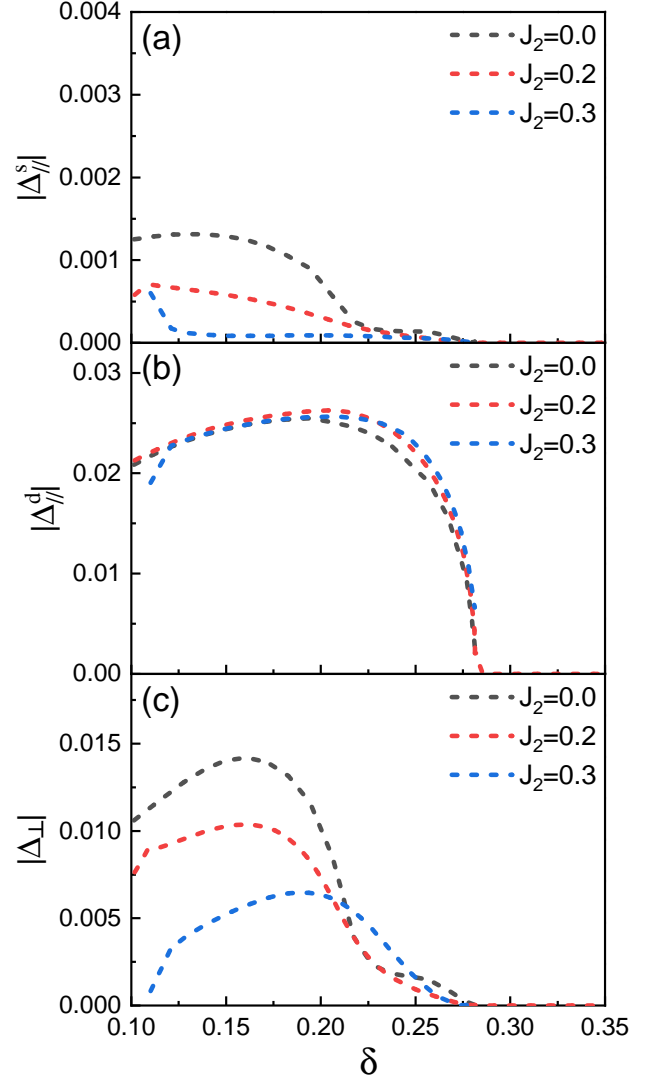


FIG. 3. Superconducting order parameter as a function of doping level with different J_2 at $t_{\perp} = 0.5, J_{\perp} = 0.3$. Superconducting order parameter for (a) intra-layer s -wave pairing, (b) intra-layer d -wave pairing, and (c) inter-layer pairing, respectively.

$$\chi_k = 2(\chi_x \cos k_x + \chi_y \cos k_y) + \chi_z \cos k_z \quad (17)$$

$$\Delta_k = 2(\Delta_x \cos k_x + \Delta_y \cos k_y) + \Delta_z \cos k_z \quad (18)$$

Following the method with [50], we use an ansatz for E_k

$$E_k = C \sqrt{\cos^2 k_x + \cos^2 k_y + \cos^2 k_z} \quad (19)$$

where C is a parameter to be determined. This ansatz gives a $s + id$ - wave pairing in xy -plane, which satisfy

$$\begin{aligned} \Delta_x &= \Delta_{s,x} + i\Delta_{d,x} \\ \Delta_y &= \Delta_{s,y} + i\Delta_{d,y} = \Delta_{s,x} - i\Delta_{d,x} \\ \Delta_d^2 - \Delta_s^2 &= \chi_x^2 = \chi_y^2 \end{aligned} \quad (20)$$

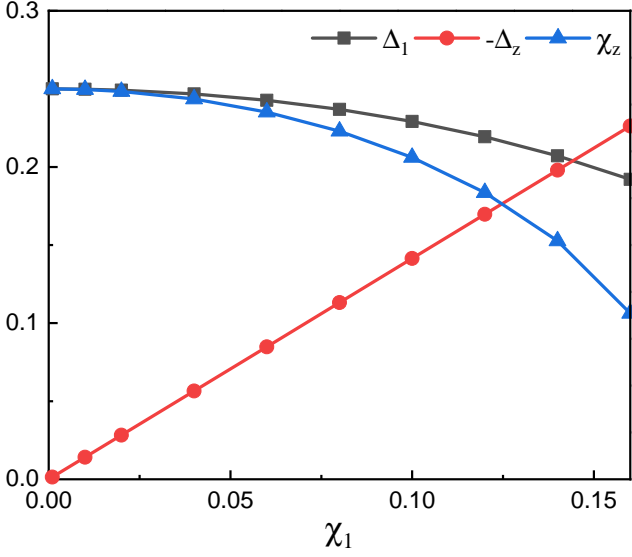


FIG. 4. The mean field $\Delta_1, \Delta_z, \chi_z$ as a function of χ_1 at half filling. Each point is a degenerate state and satisfies the constraints Eq.(22).

the inter-layer mean fields

$$\begin{aligned} 2\chi_x\chi_z + (\Delta_z\Delta_x^* + \Delta_x\Delta_z^*) &= 0 \\ 2\chi_y\chi_z + (\Delta_z\Delta_y^* + \Delta_y\Delta_z^*) &= 0 \\ \chi_x\chi_z + \Delta_z\Delta_s &= 0 \end{aligned} \quad (21)$$

The mean fields satisfy the following simultaneous equations:

$$\begin{aligned} \chi_1^2 + \Delta_1^2 &= \chi_z^2 + \Delta_z^2 = C^2 \\ \Delta_d^2 - \Delta_s^2 &= \chi_1^2 \\ \chi_1\Delta_1 &= \chi_z\Delta_s \end{aligned} \quad (22)$$

where

$$\begin{aligned} \chi_1 &= \chi_x = \chi_y, \\ \Delta_1 &= \Delta_s + i\Delta_d, \end{aligned} \quad (23)$$

We remark that there is only one independent field for fixed C . For example, if we fix χ_1 , the absolute values of all mean fields are determined. We can obtain many degenerate states by changing χ_1 . To verify this result, we solve the mean-field Hamiltonian Eq.(7) at half filling and obtain some states with the same energy as shown in Fig.4. The inter-layer pairing field Δ_z increases with the increasing of χ_1 , while intra-layer pairing field Δ_1 and inter-layer χ_z field decrease. Each point is a degenerate state, which satisfies the constraints Eq.(22).

When slightly doping holes, the above constraints are still valid. If we fix the intra-layer hopping t and raise the inter-layer hopping t_\perp from zero, χ_z increase to enhance the absolute value of inter-layer kinetic momentum, but χ_1 decreases at the same time, which will lower intra-layer kinetic momentum and leads to a smaller absolute

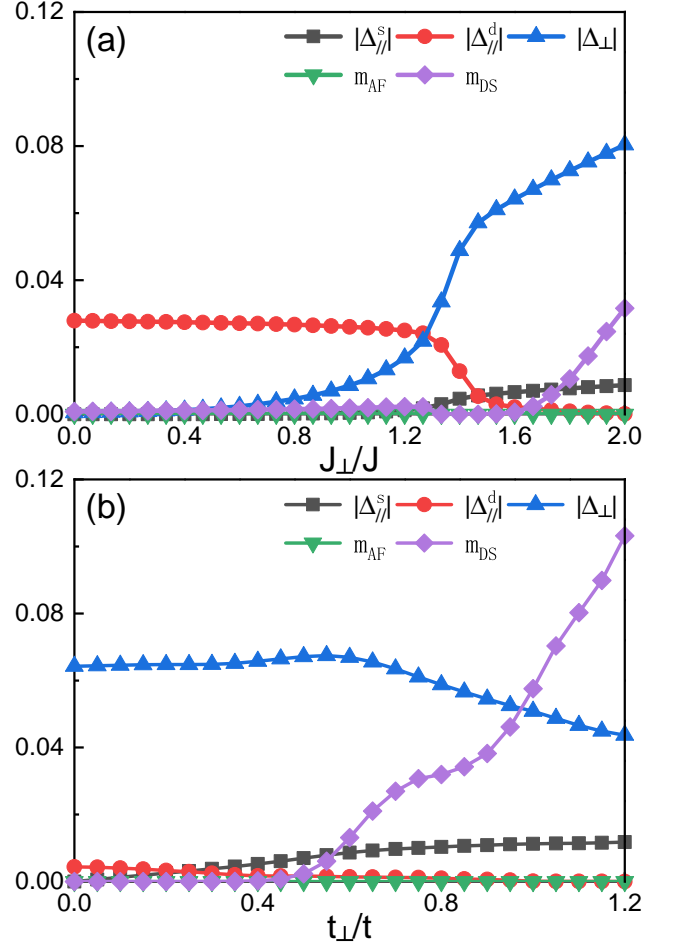


FIG. 5. (a) Superconducting order parameter and magnetic order parameter as a function of J_\perp/J_1 with doping $\delta = 0.2$ for $t_\perp = 0.5$. (b) Superconducting order parameter and magnetic order parameter as a function of t_\perp/t_1 with doping $\delta = 0.2$ for $J_\perp = 0.5$.

value of total kinetic momentum. Because t_\perp is small from the beginning, the contribution of the inter-layer kinetic energy is small, and the χ_1 is dominant. There is no obvious change at small t_\perp . When t_\perp keeps growing, χ_z will increase gradually and Δ_z decrease, Δ_1 (actually is Δ_s) increases. RMFT result in Fig.5(b) also supports this analysis.

D. Effects of J_\perp and t_\perp

In this section, we briefly discuss the effects of inter-layer hopping and coupling. According to our analysis before, the inter-layer pairing strength would increase with J_\perp/J_1 because it directly comes from the mean-field decoupling of the antiferromagnetic interaction J_\perp as shown in Fig.5(a). The intra-layer d -wave pairing $\Delta_||^d$ decreases with the increasing of J_\perp/J_1 due to the com-

petition with the inter-layer pairing Δ_{\perp} . The electron at site i chooses NN intra-layer or inter-layer electrons to form a Cooper pair. The inter-layer s -wave pairing comes from the common effect between t_{\perp} and J_{\perp} . It competes with intra-layer d -wave pairing and increases monotonically with J_{\perp}/J_1 . The bilayer structure is significant to the double spin stripe. Although it is an in-plane stripe, the corresponding magnetic order parameter m_{DS} increases with J_{\perp}/J_1 and t_{\perp}/t . The inter-layer pairing Δ_z barely changes with t_{\perp}/t in the $0 < t_{\perp}/t < 0.55$ and obviously decreases when t_{\perp} continue to increase. The intra-layer d -wave pairing and s -wave pairing monotonously decrease and increase with t_{\perp}/t , respectively, enhancing the total intra-layer pairing. Those RMFT results are consistent with the conclusion of momentum-space analysis. Those RMFT results are consistent with the conclusion of momentum-space analysis.

IV. CONCLUSION

In this work, we investigate the interplay between superconductivity and magnetism within a single-band bilayer t - J model, proposing an intra-layer $s + id$ -wave pairing and a dominant inter-layer pairing. The analysis of pairing symmetry indicates a unified solution with numerical results. The intra-layer d -wave pairing coexists with antiferromagnetism (AFM), and the intra-layer $s - wave$ pairing coexists with a double spin stripe. The transition between these states is tuned by inter-layer hopping t_{\perp} and inter-layer coupling J_{\perp} . Compared with previous theoretical studies, we consider the magnetism and identify the double spin stripe, which is anticipated by experiments. Furthermore, we propose a coexistence state of superconductivity and the double spin stripe, highlighting its evolution with t_{\perp} and J_{\perp} , which significantly increase under varying pressure. The variation in the amplitude of superconductivity with changes in interlayer parameters aligns with experimental findings.

There are some predictions about the double spin stripe in bilayer $\text{La}_3\text{Ni}_2\text{O}_7$ at ambient pressure[10, 13, 14, 46, 47], the density wave is suppressed by pressure which can enhance superconductivity. But a result of

μsR shows that the magnetic ordering temperature was observed to rise under increasing pressure[15]. Recently, an ultrafast optical pump-probe spectroscopy experiment reported a pressure-induced separation between two density wave-like orders[18], which is in agreement with the first-principles calculations[41]. They found the magnetic order aligns with the critical temperature associated with the density wave anomaly. The above two experiments confirm our numerical results in some ways. However, some problems remain to be solved: (a) Our findings demonstrate that pressure enhances the spin density wave and superconductivity in their coexisting region. However, experimental evidence indicates that the enhancement of pressure on magnetic order is confined to a narrow range around ambient pressure, and superconductivity does not appear[15]. (b) we note that within the model employed in the present paper, we have not considered the effects of the interplay between $d_{x^2-y^2}$ orbital and d_{z^2} orbital. Moreover, there might be self-doping effect between these two orbitals[27–31], which can affect the hole concentration of $d_{x^2-y^2}$ orbitals. We believe that the absence of the CDW may be related to the single orbital. Because the alternating charge distribution between Ni^{2+} and Ni^{3+} ions involves in both eg orbitals. Specifically, Ni^{2+} sites are characterized by one hole residing in the $d_{x^2-y^2}$ orbital and another in the d_{z^2} orbital, whereas Ni^{3+} sites correspond to two holes in the $d_{x^2-y^2}$ orbital and the third one in the d_{z^2} orbital. Whether CDW exists in the superconducting state needs further investigations. However, it is unequivocal that our research offers theoretical support for the coexistence of SDW and superconductivity, which may provide a key insight into the relevance between superconductivity and magnetic order.

ACKNOWLEDGEMENTS

We are grateful to Ting-Kuo Lee for many useful discussions. This work is supported by the National Key Research and Development Program of China Grant No. 2022YFA1404204, and the National Natural Science Foundation of China Grant No. 12274086.

-
- [1] S. Hualei, M. Huo, X. Hu, J. Li, Z. Liu, Y. Han, L. Tang, Z. Mao, P. Yang, B. Wang, J. Cheng, D.-X. Yao, G.-M. Zhang, and M. Wang, *Nature* **621**, 493 (2023).
 [2] Y. Zhang, D. Su, Y. Huang, Z. Shan, H. Sun, M. Huo, K. Ye, J. Zhang, Z. Yang, Y. Xu, Y. Su, R. Li, M. Smidman, M. Wang, L. Jiao, and H. Yuan, *Nature Physics* **20**, 1269 (2024).
 [3] P. Puphal, P. Reiss, N. Enderlein, Y.-M. Wu, G. Khalullin, V. Sundaramurthy, T. Priessnitz, M. Knauff, A. Suthar, L. Richter, M. Isobe, P. A. van Aken, H. Takagi, B. Keimer, Y. E. Suyolcu, B. Wehinger, P. Hansmann, and M. Hepting, *Phys. Rev. Lett.* **133**, 146002

- (2024).
 [4] G. Wang, N. N. Wang, X. L. Shen, J. Hou, L. Ma, L. F. Shi, Z. A. Ren, Y. D. Gu, H. M. Ma, P. T. Yang, Z. Y. Liu, H. Z. Guo, J. P. Sun, G. M. Zhang, S. Calder, J.-Q. Yan, B. S. Wang, Y. Uwatoko, and J.-G. Cheng, *Phys. Rev. X* **14**, 011040 (2024).
 [5] Y. Zhu, D. Peng, E. Zhang, B. Pan, X. Chen, L. Chen, H. Ren, F. Liu, Y. Hao, N. Li, Z. Xing, F. Lan, J. Han, J. Wang, D. Jia, H. Wo, Y. Gu, Y. Gu, L. Ji, W. Wang, H. Gou, Y. Shen, T. Ying, X. Chen, W. Yang, H. Cao, C. Zheng, Q. Zeng, J. gang Guo, and J. Zhao, *Nature* **631**, 531 (2024).

- [6] M. Kakoi, T. Oi, Y. Ohshita, M. Yashima, K. Kuroki, T. Kato, H. Takahashi, S. Ishiwata, Y. Adachi, N. Hatada, T. Uda, and H. Mukuda, *Journal of the Physical Society of Japan* **93**, 053702 (2024).
- [7] H. Sakakibara, M. Ochi, H. Nagata, Y. Ueki, H. Sakurai, R. Matsumoto, K. Terashima, K. Hirose, H. Ohta, M. Kato, Y. Takano, and K. Kuroki, *Phys. Rev. B* **109**, 144511 (2024).
- [8] Q. Li, Y.-J. Zhang, Z.-N. Xiang, Y. Zhang, X. Zhu, and H.-H. Wen, *Chinese Physics Letters* **41**, 017401 (2024).
- [9] M. Zhang, C. Pei, X. Du, W. Hu, Y. Cao, Q. Wang, J. Wu, Y. Li, H. Liu, C. Wen, Y. Zhao, C. Li, W. Cao, S. Zhu, Q. Zhang, N. Yu, P. Cheng, L. Zhang, Z. Li, J. Zhao, Y. Chen, H. Guo, C. Wu, F. Yang, S. Yan, L. Yang, and Y. Qi, *Superconductivity in trilayer nickelate $\text{La}_4\text{Ni}_3\text{O}_{10}$ under pressure* (2024), [arXiv:2311.07423](https://arxiv.org/abs/2311.07423) [cond-mat.supr-con].
- [10] X. Chen, J. Choi, Z. Jiang, J. Mei, K. Jiang, J. Li, S. Agrestini, M. Garcia-Fernandez, X. Huang, H. Sun, D. Shen, M. Wang, J. Hu, Y. Lu, K.-J. Zhou, and D. Feng, *Nature Communications* **15**, 10.1038/s41467-024-53863-5 (2024).
- [11] T. Xie, M. Huo, X. Ni, F. Shen, X. Huang, H. Sun, H. C. Walker, D. Adroja, D. Yu, B. Shen, L. He, K. Cao, and M. Wang, *Science Bulletin* **69**, 3221 (2024).
- [12] Z. Dan, Y. Zhou, M. Huo, Y. Wang, L. Nie, M. Wang, T. Wu, and X. Chen, *Spin-density-wave transition in double-layer nickelate $\text{La}_3\text{Ni}_2\text{O}_7$* (2024), [arXiv:2402.03952](https://arxiv.org/abs/2402.03952) [cond-mat.supr-con].
- [13] N. K. Gupta, R. Gong, Y. Wu, M. Kang, C. T. Parzyck, B. Z. Gregory, N. Costa, R. Sutarto, S. Sarker, A. Singer, D. G. Schlom, K. M. Shen, and D. G. Hawthorn, *Anisotropic spin stripe domains in bilayer $\text{La}_3\text{Ni}_2\text{O}_7$* (2024), [arXiv:2409.03210](https://arxiv.org/abs/2409.03210) [cond-mat.supr-con].
- [14] K. Chen, X. Liu, J. Jiao, M. Zou, C. Jiang, X. Li, Y. Luo, Q. Wu, N. Zhang, Y. Guo, and L. Shu, *Phys. Rev. Lett.* **132**, 256503 (2024).
- [15] R. Khasanov, T. J. Hicken, D. J. Gawryluk, L. P. Sorel, S. Bötzel, F. Lechermann, I. M. Eremin, H. Luetkens, and Z. Guguchia, *Pressure-induced split of the density wave transitions in $\text{La}_3\text{Ni}_2\text{O}_{7-\delta}$* (2024), [arXiv:2402.10485](https://arxiv.org/abs/2402.10485) [cond-mat.supr-con].
- [16] J. Liao, K. Ruttik, R. Jantti, and P.-H. Dinh-Thuy, *Coded backscattering communication with lte pilots as ambient signal* (2024), [arXiv:2402.12657](https://arxiv.org/abs/2402.12657) [eess.SP].
- [17] A. K. Mirabadi, G. Archibald, A. Darbandsari, A. Contreras-Sanz, R. E. Nakhli, M. Asadi, A. Zhang, C. B. Gilks, P. Black, G. Wang, H. Farahani, and A. Bashashati, *Grasp: Graph-structured pyramidal whole slide image representation* (2024), [arXiv:2402.03592](https://arxiv.org/abs/2402.03592) [cs.CV].
- [18] Y. Meng, Y. Yang, H. Sun, S. Zhang, J. Luo, M. Wang, F. Hong, X. Wang, and X. Yu, *Nature Communications* **15**, 10.1038/s41467-024-54518-1 (2024).
- [19] Z. Luo, X. Hu, M. Wang, W. Wú, and D.-X. Yao, *Phys. Rev. Lett.* **131**, 126001 (2023).
- [20] Y. Zhang, L.-F. Lin, A. Moreo, and E. Dagotto, *Phys. Rev. B* **108**, L180510 (2023).
- [21] X. Chen, P. Jiang, J. Li, Z. Zhong, and Y. Lu, *Critical charge and spin instabilities in superconducting $\text{La}_3\text{Ni}_2\text{O}_7$* (2023), [arXiv:2307.07154](https://arxiv.org/abs/2307.07154) [cond-mat.supr-con].
- [22] F. Lechermann, J. Gondolf, S. Bötzel, and I. M. Eremin, *Phys. Rev. B* **108**, L201121 (2023).
- [23] V. Christiansson, F. Petocchi, and P. Werner, *Phys. Rev. Lett.* **131**, 206501 (2023).
- [24] Y. Gu, C. Le, Z. Yang, X. Wu, and J. Hu, *Effective model and pairing tendency in bilayer ni-based superconductor $\text{La}_3\text{Ni}_2\text{O}_7$* (2023), [arXiv:2306.07275](https://arxiv.org/abs/2306.07275) [cond-mat.supr-con].
- [25] Q.-G. Yang, D. Wang, and Q.-H. Wang, *Phys. Rev. B* **108**, L140505 (2023).
- [26] Y.-B. Liu, J.-W. Mei, F. Ye, W.-Q. Chen, and F. Yang, *Phys. Rev. Lett.* **131**, 236002 (2023).
- [27] Y.-f. Yang, G.-M. Zhang, and F.-C. Zhang, *Phys. Rev. B* **108**, L201108 (2023).
- [28] H. Sakakibara, N. Kitamine, M. Ochi, and K. Kuroki, *Phys. Rev. Lett.* **132**, 106002 (2024).
- [29] Y. Shen, M. Qin, and G.-M. Zhang, *Chinese Physics Letters* **40**, 127401 (2023).
- [30] X.-Z. Qu, D.-W. Qu, J. Chen, C. Wu, F. Yang, W. Li, and G. Su, *Phys. Rev. Lett.* **132**, 036502 (2024).
- [31] Y. Cao and Y.-f. Yang, *Phys. Rev. B* **109**, L081105 (2024).
- [32] Y.-H. Tian, Y. Chen, J.-M. Wang, R.-Q. He, and Z.-Y. Lu, *Phys. Rev. B* **109**, 165154 (2024).
- [33] D.-C. Lu, M. Li, Z.-Y. Zeng, W. Hou, J. Wang, F. Yang, and Y.-Z. You, *Superconductivity from doping symmetric mass generation insulators: Application to $\text{La}_3\text{Ni}_2\text{O}_7$ under pressure* (2023), [arXiv:2308.11195](https://arxiv.org/abs/2308.11195) [cond-mat.str-el].
- [34] J. Huang, Z. D. Wang, and T. Zhou, *Phys. Rev. B* **108**, 174501 (2023).
- [35] R. Jiang, J. Hou, Z. Fan, Z.-J. Lang, and W. Ku, *Phys. Rev. Lett.* **132**, 126503 (2024).
- [36] Z. Liao, L. Chen, G. Duan, Y. Wang, C. Liu, R. Yu, and Q. Si, *Phys. Rev. B* **108**, 214522 (2023).
- [37] C. Lu, Z. Pan, F. Yang, and C. Wu, *Phys. Rev. Lett.* **132**, 146002 (2024).
- [38] H. Oh and Y.-H. Zhang, *Phys. Rev. B* **108**, 174511 (2023).
- [39] Q. Qin and Y.-f. Yang, *Phys. Rev. B* **108**, L140504 (2023).
- [40] D. A. Shilenko and I. V. Leonov, *Phys. Rev. B* **108**, 125105 (2023).
- [41] X.-W. Yi, Y. Meng, J.-W. Li, Z.-W. Liao, W. Li, J.-Y. You, B. Gu, and G. Su, *Phys. Rev. B* **110**, L140508 (2024).
- [42] T. Kaneko, H. Sakakibara, M. Ochi, and K. Kuroki, *Phys. Rev. B* **109**, 045154 (2024).
- [43] C. Qin, K. Foyevtsova, L. Si, G. A. Sawatzky, and M. Jiang, *Intertwined charge and spin density wave state of $\text{La}_3\text{Ni}_2\text{O}_7$* (2024), [arXiv:2410.15649](https://arxiv.org/abs/2410.15649) [cond-mat.supr-con].
- [44] H.-Y. Zhang, Y.-J. Bai, F.-J. Kong, X.-Q. Wu, Y.-H. Xing, and N. Xu, *Doping evolution of the normal state magnetic excitations in pressurized $\text{La}_3\text{Ni}_2\text{O}_7$* (2024), [arXiv:2408.03763](https://arxiv.org/abs/2408.03763) [cond-mat.supr-con].
- [45] Y. Zhang, L.-F. Lin, A. Moreo, T. A. Maier, and E. Dagotto, *Nature Communications* **15**, 10.1038/s41467-024-46622-z (2024).
- [46] H. LaBollita, V. Pardo, M. R. Norman, and A. S. Botana, *Assessing the formation of spin and charge stripes in $\text{La}_3\text{Ni}_2\text{O}_7$ from first-principles* (2024), [arXiv:2407.14409](https://arxiv.org/abs/2407.14409) [cond-mat.str-el].
- [47] B. Zhang, C. Xu, and H. Xiang, *Emergent spin-charge-orbital order in superconductor $\text{La}_3\text{Ni}_2\text{O}_7$* (2024), [arXiv:2407.18473](https://arxiv.org/abs/2407.18473) [cond-mat.supr-con].

- [48] L.-F. Lin, Y. Zhang, N. Kaushal, G. Alvarez, T. A. Maier, A. Moreo, and E. Dagotto, [Magnetic phase diagram of a two-orbital model for bilayer nickelates varying doping \(2024\)](#), [arXiv:2408.05689 \[cond-mat.str-el\]](#).
- [49] F. Zhang, C. Gros, T. Rice, and H. Shiba, [Superconductor Science and Technology](#) **1** (2003).
- [50] M. Ogata and A. Himeda, [Journal of The Physical Society of Japan - J PHYS SOC JPN](#) **72**, 374 (2003).
- [51] M. Sgrist, T. M. Rice, and F. C. Zhang, [Phys. Rev. B](#) **49**, 12058 (1994).
- [52] J. Hou, T.-K. Lee, Y. Guo, J. Lou, and Y. Chen, [New Journal of Physics](#) **21**, 113047 (2019).
- [53] F. C. Zhang and T. M. Rice, [Phys. Rev. B](#) **37**, 3759 (1988).
- [54] Y. Gu, C. Le, Z. Yang, X. Wu, and J. Hu, [Effective model and pairing tendency in bilayer ni-based superconductor \$\text{la}_3\text{ni}_2\text{o}_7\$ \(2023\)](#), [arXiv:2306.07275 \[cond-mat.supr-con\]](#).
- [55] Y. Zhang, L.-F. Lin, A. Moreo, T. A. Maier, and E. Dagotto, [Phys. Rev. B](#) **108**, 165141 (2023).